The 17th Annual IEEE International Symposium on Personal, Indoor and Mobile Radio Communications (PIMRC'06)

KRYLOV SUBSPACE METHOD BASED LOW-COMPLEXITY MIMO MULTI-USER RECEIVER FOR TIME-VARIANT CHANNELS

Charlotte Dumard and Thomas Zemen
ftw. Forschungzentrum Telekommunikation Wien
Donau-City-Strasse 1/3, A-1220 Vienna
Austria
{ **dumard**, thomas.zemen} @ftw.at

ABSTRACT

We consider the uplink of a time-variant multiple-input-multiple-output (MIMO) multi-user (MU) multi-carrier (MC) code division multiple access (CDMA) system. The linear minimum mean square error (LMMSE) filters for channel estimation and multi-user detection at the receiver side require too high complexity to be implementable in a system operating in time-variant channels. We develop a low-complexity implementation of an LMMSE filter based on the Krylov subspace method. We are able to reduce the computational complexity by one order of magnitude. Furthermore, in a system with K users having N_T transmit antennas, parallelization of the computations of the multi-user detector into KN_T branches is achieved as well as considerable storage reduction. We discuss more specifically a fully loaded system (the number of subcarriers N is equal to the number of users K) with $N_T = 2$ transmit antennas per user, $N_R = 4$ receive antennas and $K = N = 64$.

I. INTRODUCTION

Exact LMMSE filters are difficult to implement in a real-time system. We develop a low-complexity algorithm based on Krylov subspace methods [7, 8] to approximate an LMMSE filter, trading accuracy for efficiency. Convergence of the iterative Krylov algorithm can be accelerated by choosing a suitable starting value [2]. In this paper we extend previous results obtained for a single-input-single-output (SISO) MU system [1,2] to a MIMO-MU system [5]. We consider independent or joint coding at each transmitter and independent or joint antenna detection at the receiver.

Our contribution: We implement the single and joint antenna detectors and the channel estimator using the Krylov subspace method. We discuss their performance in a fully loaded system with K users, where each transmitter uses independent or joint coding for its N_T transmit antennas. The multi-user receiver based on the Krylov subspace method achieves computational complexity reduction by one order of magnitude as well as parallelization of the multi-user detection into KN_T branches.

The paper is organized as follows: We describe the multi-antenna transmitter in Section II. and the multi-antenna iterative receiver in Section III. We briefly review the integration of the Krylov method in the iterative receiver in Section IV. The computational complexity is discussed in Section V. Simulation results are presented in Section VI. and conclusions are drawn in Section VII.

II. MULTI-ANTENNA TRANSMITTER

We extend the system described in [5, 9] to a multi-antenna transmitter. Each user $k \in \{1, \ldots, K\}$ has $N_T \geq 1$ transmit antennas. The MC-CDMA uplink transmission is based on orthogonal frequency division multiplexing (OFDM) with N subcarriers. We consider the transmission of N_T data blocks, each of them consisting of $M - J$ OFDM data symbols and J OFDM pilot symbols. Each antenna $t \in \{1, \ldots, N_T\}$ of each user k transmits symbols $b_{k,t}[m]$[1] with symbol rate $1/T_\mathrm{S}$. The discrete time index is denoted by m. Each symbol is spread by a random spreading sequence $\boldsymbol{s}_{k,t} \in \mathbb{C}^N$ with independent identically distributed (i.i.d.) elements chosen from the set $\{\pm 1 \pm \mathrm{j}\}/\sqrt{2N}$.

The $M - J$ data symbols are distributed over a block of length M fulfilling $b_{k,t}[m] \in \{\pm 1 \pm \mathrm{j}\}/\sqrt{2}$ for $m \notin \mathcal{P}$ and $b_{k,t}[m] = 0$ for $m \in \mathcal{P}$, allowing for pilot symbol insertion. The pilot placement is defined through the index set

$$\mathcal{P} = \left\{ \left\lfloor i\frac{M}{J} + \frac{M}{2J} \right\rfloor \;\middle|\; i \in \{0, \ldots, J-1\} \right\} . \qquad (1)$$

After spreading, pilot symbols $\boldsymbol{p}_{k,t}[m] \in \mathbb{C}^N$ are added

$$\boldsymbol{d}_{k,t}[m] = \boldsymbol{s}_{k,t} b_{k,t}[m] + \boldsymbol{p}_{k,t}[m] . \qquad (2)$$

The elements of the pilot symbols $p_{k,t}[m,q]$ for $m \in \mathcal{P}$ and $q \in \{0, \ldots, N-1\}$ are randomly chosen from the QPSK symbol set $\{\pm 1 \pm \mathrm{j}\}/\sqrt{2N}$, otherwise $\boldsymbol{p}_{k,t}[m] = \mathbf{0}_N$.

We consider two modes of encoding, using a convolutional, non-systematic, non-recursive, 4 state, rate $R_C = 1/2$ code with generator polynomial $(5, 7)_8$:

- **Independent Encoding:** The N_T data blocks are independently encoded, interleaved, mapped to the QPSK constellation, spread and transmitted. The corresponding transmitter structure is shown in Fig. 1.
- **Joint Encoding:** The N_T data blocks are jointly encoded, interleaved and mapped. Then the $N_T(M - J)$ coded symbols are split into N_T coded symbol blocks that are independently spread and transmitted. The corresponding transmitter structure is shown in Fig. 2.

[1]Notation: We denote a column vector with elements $a[i]$ by $\boldsymbol{a}$, and a matrix with elements $[\boldsymbol{A}]_{i,j}$ by $\boldsymbol{A}$. The k-th column of $\boldsymbol{A}$ is denoted $\boldsymbol{A}_k$. The transpose (conjugate transpose) of a matrix or vector is denoted through $\cdot^\mathrm{T}$ $(\cdot^\mathrm{H})$. A diagonal matrix with elements $a[i]$ is written as $\mathrm{diag}(\boldsymbol{a})$ and the $Q \times Q$ identity matrix as $\boldsymbol{I}_Q$. The vector of size Q containing zeros is denoted $\mathbf{0}_Q$. The norm of $\boldsymbol{a}$ is denoted through $\|\boldsymbol{a}\|$ and its norm with respect to a matrix $\boldsymbol{A}$ through $\|\boldsymbol{a}\|_{\boldsymbol{A}} = \sqrt{\boldsymbol{a}^\mathrm{H}\boldsymbol{A}\boldsymbol{a}}$. The largest integer, lower than or equal to $b \in \mathbb{R}$ is denoted by $\lfloor b \rfloor$. The superscript (i) denotes the i-th iteration of the receiver.

For each transmit antenna an N-point inverse discrete Fourier transform (DFT) is performed and a cyclic prefix of length G is inserted. A single OFDM symbol together with the cyclic prefix has length $P = N + G$ chips. After parallel to serial conversion the chip stream with chip rate $1/T_{\mathrm{C}} = P/T_{\mathrm{S}}$ is transmitted over a time-variant multipath fading channel with L resolvable paths.

III. Multi-antenna Receiver

The receiver has $N_R \geq 1$ receive antennas. At each receive antenna $r \in \{1, \ldots, N_R\}$, the signals of all KN_T transmit antennas add up. In the receiver, the transmission encoding scheme is taken into account by appropriate demapping, deinterleaving and decoding. At each antenna, the cyclic prefix is removed and a DFT is performed. The received signal vector $\boldsymbol{y}_r[m] \in \mathbb{C}^N$ at receive antenna r after these two operations is given by

$$\boldsymbol{y}_r[m] = \sum_{k=1}^{K} \sum_{t=1}^{N_T} \operatorname{diag}\left(\boldsymbol{g}_{k,t,r}[m]\right) \boldsymbol{d}_{k,t}[m] + \boldsymbol{z}_r[m]\,, \quad (3)$$

where complex additive white Gaussian noise with zero mean and covariance $\sigma_z^2 \boldsymbol{I}_N$ is denoted by $\boldsymbol{z}_r[m] \in \mathbb{C}^N$ with elements $z_r[m, q]$. The time-variant frequency response between transmit antenna t of user k and receive antenna r is denoted by $\boldsymbol{g}_{k,t,r} \in \mathbb{C}^N$. All channels $\boldsymbol{g}_{k,t,r}$ are assumed uncorrelated. Thus each receive antenna performs channel estimation independently. We define $\hat{\boldsymbol{g}}_{k,t,r}[m]$ as the channel estimate at discrete time m of the time-variant channel $\boldsymbol{g}_{k,t,r}$. For channel estimation we use a subspace spanned by discrete prolate spheroidal (DPS) sequences with dimension $D << M$. For practical mobile communications systems, $D \leq 5$, see [10]. The reduced complexity of the time-variant channel estimator using the Krylov subspace method is detailed in [1].

The effective spreading sequence at time m is

$$\tilde{\boldsymbol{s}}_{k,t,r}[m] = \operatorname{diag}\left(\hat{\boldsymbol{g}}_{k,t,r}[m]\right) \boldsymbol{s}_{k,t} \in \mathbb{C}^N\,. \quad (4)$$

Unless necessary, we omit now the time-index m. The time-variant effective spreading matrix at antenna r is given by

$$\tilde{\boldsymbol{S}}_r = [\tilde{\boldsymbol{s}}_{1,1,r}, \ldots, \tilde{\boldsymbol{s}}_{1,N_T,r}, \ldots, \tilde{\boldsymbol{s}}_{K,1,r}, \ldots, \tilde{\boldsymbol{s}}_{K,N_T,r}]\,. \quad (5)$$

Using these definitions the signal received at antenna r writes $\boldsymbol{y}_r = \tilde{\boldsymbol{S}}_r \boldsymbol{b} + \boldsymbol{z}_r$, where

$$\boldsymbol{b} = [b_{1,1}, \ldots, b_{1,N_T}, \ldots, b_{K,1}, \ldots, b_{K,N_T}]^{\mathrm{T}} \in \mathbb{C}^{KN_T} \quad (6)$$

contains the data symbols for the KN_T transmit antennas.

Data detection is performed using the soft symbol estimates $\tilde{b}_{k,t}$. They are computed from the extrinsic probability supplied by the decoding stage

$$\begin{aligned} \tilde{b}_{k,t}[m] = \; & \tfrac{1}{\sqrt{2}} \left(2\mathrm{EXT}(c_{k,t}[2m]) - 1\right) \\ & + \mathrm{j} \tfrac{1}{\sqrt{2}} \left(2\mathrm{EXT}(c_{k,t}[2m+1]) - 1\right)\,. \end{aligned} \quad (7)$$

We define the error covariance matrix of the soft symbols

$$\boldsymbol{V} = \mathbb{E}\{(\boldsymbol{b} - \tilde{\boldsymbol{b}})(\boldsymbol{b} - \tilde{\boldsymbol{b}})^{\mathrm{H}}\}\,, \quad (8)$$

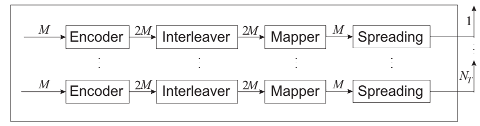

Figure 1: Independent encoding for N_T transmit antennas.

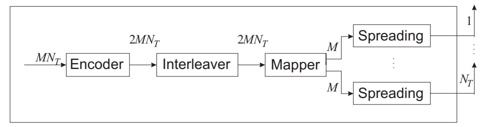

Figure 2: Joint encoding for N_T transmit antennas.

with constant diagonal elements $V_{k,t} = \mathbb{E}\{1 - |\tilde{b}_{k,t}|^2\}$ during the iteration. $\boldsymbol{b}$ and $\tilde{\boldsymbol{b}}$ are supposed to be independent and the other elements of $\boldsymbol{V}$ are assumed to be zeros.

For multi-user detection, we compare two different architectures.

A. *Single Antenna Detection*

Each antenna performs detection independently. Thus, the N_R antennas are considered as N_R independent receivers. To cancel the multi-access interference, we perform soft parallel interference cancellation (PIC) for transmit antenna t of user k at receive antenna r

$$\tilde{\boldsymbol{y}}_{k,t,r} = \boldsymbol{y}_r + \tilde{\boldsymbol{s}}_{k,t,r} \tilde{b}_{k,t} - \tilde{\boldsymbol{S}}_r \tilde{\boldsymbol{b}}\,. \quad (9)$$

The unbiased conditional LMMSE filter writes as[2]

$$\boldsymbol{f}_{k,t,r} = \frac{\left(\sigma_z^2 \boldsymbol{I}_N + \tilde{\boldsymbol{S}}_r \boldsymbol{V} \tilde{\boldsymbol{S}}_r^{\mathrm{H}}\right)^{-1} \tilde{\boldsymbol{s}}_{k,t,r}}{\tilde{\boldsymbol{s}}_{k,t,r}{}^{\mathrm{H}} \left(\sigma_z^2 \boldsymbol{I}_N + \tilde{\boldsymbol{S}}_r \boldsymbol{V} \tilde{\boldsymbol{S}}_r^{\mathrm{H}}\right)^{-1} \tilde{\boldsymbol{s}}_{k,t,r}}\,. \quad (10)$$

The output of the filter is an estimate of $b_{k,t}$ for receive antenna r expressed by

$$\hat{b}_{k,t,r} = \boldsymbol{f}_{k,t,r}^{\mathrm{H}} \tilde{\boldsymbol{y}}_{k,t,r}\,. \quad (11)$$

These N_R estimates of $b_{k,t}$ are then combined using maximum ratio combining, leading to

$$\breve{b}_{k,t} = \frac{\sum_{r=1}^{N_R} ||\hat{\boldsymbol{g}}_{k,t,r}||^2 \hat{b}_{k,t,r}}{\sum_{r=1}^{N_R} ||\hat{\boldsymbol{g}}_{k,t,r}||^2}\,. \quad (12)$$

The $\breve{b}_{k,t}$ are decoded by a BCJR decoder after demapping and deinterleaving.

B. *Joint Antenna Detection*

We investigate here the case where all N_R signals are combined in order to perform joint detection. This method has the advantage of taking into account the correlation between the received signals of all antennas, but has greater storage and computation requirements. We define the global received signal $\hat{\boldsymbol{y}}$ as the vector containing all $\boldsymbol{y}_r$ for $r \in \{1, \ldots, N_R\}$ and expressed by

$$\hat{\boldsymbol{y}} = [\boldsymbol{y}_1^{\mathrm{T}}, \ldots, \boldsymbol{y}_{N_R}^{\mathrm{T}}]^{\mathrm{T}} \in \mathbb{C}^{NN_R}\,. \quad (13)$$

[2] We are interested in a fully loaded system ($K = N$) thus $N < KN_T$. However, $\tilde{\boldsymbol{S}}_r$ has size NxKN_T and in the case $N > KN_T$, the matrix inversion lemma [6] can be applied to obtain a matrix with smaller dimensions.

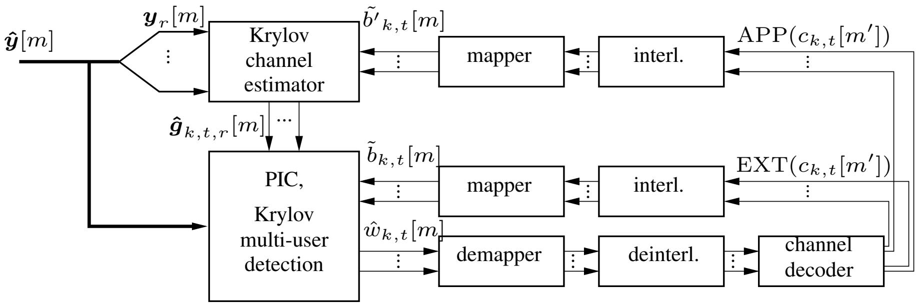

Figure 3: The MC-CDMA receiver performs iterative time-variant channel estimation jointly for all users and independently per receive antenna as well as multi-user detection jointly for all users and antennas.

Similarly, we define $\hat{\boldsymbol{S}} = [\tilde{\boldsymbol{S}}_1^{\mathrm{T}}, \ldots, \tilde{\boldsymbol{S}}_{N_R}^{\mathrm{T}}]^{\mathrm{T}} \in \mathbb{C}^{NN_R \mathrm{x} KN_T}$ and $\hat{\boldsymbol{z}} = [\boldsymbol{z}_1^{\mathrm{T}}, \ldots, \boldsymbol{z}_{N_R}^{\mathrm{T}}]^{\mathrm{T}} \in \mathbb{C}^{NN_R}$. We can rewrite $\hat{\boldsymbol{y}} = \hat{\boldsymbol{S}}\boldsymbol{b} + \hat{\boldsymbol{z}}$.

PIC for user k and transmit antenna t is performed,

$$\hat{\boldsymbol{y}}_{k,t} = \hat{\boldsymbol{y}} + \hat{\boldsymbol{s}}_{k,t}\tilde{b}_{k,t} - \hat{\boldsymbol{S}}\tilde{\boldsymbol{b}}\,, \tag{14}$$

where $\hat{\boldsymbol{s}}_{k,t}$ is the $((k-1)N_T + t)$-th column of $\hat{\boldsymbol{S}}$. We consider the case $KN_T < NN_R$. The unbiased LMMSE filter after using the matrix inversion lemma [6] writes

$$\hat{\boldsymbol{f}}_{k,t} = \frac{\hat{\boldsymbol{S}}\left(\sigma_z^2 \boldsymbol{I}_{KN_T} + \boldsymbol{V}\hat{\boldsymbol{S}}^{\mathrm{H}}\hat{\boldsymbol{S}}\right)^{-1}\hat{\boldsymbol{e}}_{k,t}}{\hat{\boldsymbol{s}}_{k,t}^{\mathrm{H}}\hat{\boldsymbol{S}}\left(\sigma_z^2 \boldsymbol{I}_{KN_T} + \boldsymbol{V}\hat{\boldsymbol{S}}^{\mathrm{H}}\hat{\boldsymbol{S}}\right)^{-1}\hat{\boldsymbol{e}}_{k,t}}\,, \tag{15}$$

where $\hat{\boldsymbol{e}}_{k,t}$ is the $(N_T(k-1)+t)$-th elementary vector. Estimates of the transmitted symbols $b_{k,t}$ are given by $\breve{b}_{k,t} = \hat{\boldsymbol{f}}_{k,t}^{\mathrm{H}}\hat{\boldsymbol{y}}_{k,t}$ and decoded by a BCJR decoder, after demapping and deinterleaving.

In Fig. 3 we show the MIMO-MU receiver for joint antenna detection. In case of single antenna detection, the receiver performs PIC and multi-user detection for each receive antenna independently.

IV. The Krylov Subspace Method

Krylov subspace methods [7, 8] approximate the solution of a linear system $\boldsymbol{A}\boldsymbol{x} = \boldsymbol{a}$ where $\boldsymbol{A}$ is a known matrix with size $Q \times Q$ and $\boldsymbol{a}$ is a known vector with size $Q \times 1$. We consider the Conjugate Gradient algorithm [7], developped for hermitian matrices. An initial value $\boldsymbol{x}_0$ is projected onto $\mathcal{K}_s = \mathrm{span}\left\{\tilde{\boldsymbol{a}}, \boldsymbol{A}\tilde{\boldsymbol{a}}, \ldots, \boldsymbol{A}^{s-1}\tilde{\boldsymbol{a}}\right\}$, known as Krylov subspace of $\boldsymbol{A}$ and $\tilde{\boldsymbol{a}}$ of dimension s, where $\tilde{\boldsymbol{a}} = \boldsymbol{a} - \boldsymbol{A}\boldsymbol{x}_0$. The algorithm iteratively computes an approximate solution at step s denoted through $\boldsymbol{x}_s$ [1, 2].

An upper bound of the error $\|\boldsymbol{x}_s - \boldsymbol{x}\|_{\boldsymbol{A}}$ at step s is [4]

$$\|\boldsymbol{x}_s - \boldsymbol{x}\|_{\boldsymbol{A}} \leq 2\|\boldsymbol{x}_0 - \boldsymbol{x}\|_{\boldsymbol{A}}\left(\frac{\sqrt{k_{\boldsymbol{A}}}-1}{\sqrt{k_{\boldsymbol{A}}}+1}\right)^s, \tag{16}$$

where the condition number $k_{\boldsymbol{A}} = \frac{\lambda_{\max}(\boldsymbol{A})}{\lambda_{\min}(\boldsymbol{A})} > 1$ of matrix $\boldsymbol{A}$ is defined as the ratio of its largest to its smallest eigenvalue. Hence convergence is assured ($\frac{\sqrt{k_{\boldsymbol{A}}}-1}{\sqrt{k_{\boldsymbol{A}}}+1} < 1$), but the convergence speed depends strongly on the spectrum of $\boldsymbol{A}$ and the choice of $\boldsymbol{x}_0$.

Implementing the Krylov subspace method to approximate (10) or (15) is equivalent to approximating $\boldsymbol{A}^{-1}\boldsymbol{a}$, where $\boldsymbol{A}$ and $\boldsymbol{a}$ are defined as follows depending on the detector

- Single Antenna Detector (SAD)

$$\boldsymbol{A}_r^{\mathrm{SAD}} = \sigma_z^2 \boldsymbol{I}_N + \tilde{\boldsymbol{S}}_r \boldsymbol{V}\tilde{\boldsymbol{S}}_r^{\mathrm{H}} \quad \boldsymbol{a}_{k,t,r}^{\mathrm{SAD}} = \tilde{\boldsymbol{s}}_{k,t,r} \tag{17}$$

- Joint Antenna Detector (JAD)

$$\boldsymbol{A}^{\mathrm{JAD}} = \sigma_z^2 \boldsymbol{I}_{KN_T} + \boldsymbol{V}\hat{\boldsymbol{S}}^{\mathrm{H}}\hat{\boldsymbol{S}} \quad \boldsymbol{a}_{k,t}^{\mathrm{JAD}} = \hat{\boldsymbol{e}}_{k,t} \tag{18}$$

From Equation (16), we see that a suitable starting value $\boldsymbol{x}_0$ may accelerate the convergence of the Krylov algorithm. We develop several initialization methods in [2]:

- The **time** method allows adaptation from symbol to symbol. The starting value at symbol $m+1$ is the result obtained at the previous symbol m. This method is available for multi-user detection.
- The **loop** method allows adaptation from receiver iteration to receiver iteration. The starting value at iteration $(i+1)$ is the result obtained at the previous iteration (i). This method is available for channel estimation. It is possible for multi-user detection also, but performs slightly worse than the **time** method [2]. Thus this situation is not considered here.

The Krylov subspaces dimensions are varied along this work.

V. On the Computational Complexity

The approximate computational complexity results are given in number of complex multiplications (CM) required. We remind that N is the number of subcarriers, M the number of symbols (including pilot symbols) over a block, D is the DPS subspace dimension for channel estimation and S and S' are the Krylov subspace dimension for multi-user detection (MUD) and channel estimation (CE) respectively. We recall the results detailed in [1] for a SISO-MU system that we will extend to a MIMO-MU system

SISO-MU	Exact LMMSE	Krylov
CE	$(\frac{2}{3}KD + M)(KD)^2$	$2S'MKD$
MUD	$2N^2(K + \frac{1}{3}N)$	$SKN(2K+7)$

From a MIMO receiver point-of-view, K users with N_T antennas act like KN_T virtual users. Thus, the dimension K in the SISO equations is simply replaced by KN_T. The influence of the number of receive antennas N_R is more complex and depends on the type of receiver.

A. *Channel Estimation (CE)*

Regardless of the receiver type, channel estimation is performed similarly. Since all channels are assumed uncorrelated, each receive antenna has its own channel estimator. Thus the MIMO-MU channel estimator acts like N_R independent estimators and the computational complexity is N_R times the one of the SISO case.

B. *Multi-User Detection*

Here we need to make the distinction between the single antenna and the joint antenna detectors. We consider a fully loaded system ($K = N$) with $N_T \leq N_R$, thus $N \leq KN_T$ and $KN_T \leq NN_R$[3].

Single Antenna Detector (SAD): Every receive antenna r acts independently and has its own effective spreading and Krylov matrices. The computational complexity for single antenna detection (SAD) is N_R times the one of the SISO case.

Joint Antenna Detector (JAD): A CDMA system with spreading factor N and N_R receive antennas behaves like a single antenna system with spreading factor NN_R (*resource pooling* result, see [3]). Thus we replace the dimension N in the previous equation by NN_R.

The expressions for computational complexity of a MIMO-MU system are summarized here[4]

MIMO-MU	Exact LMMSE
CE	$(\frac{2}{3}KN_TD + M + N_R)(KN_TD)^2$
SAD	$2N_RN^2(KN_T + \frac{1}{3}N)$
JAD	$2(KN_T)^2\left(NN_R + \frac{1}{3}KN_T\right)$
	Krylov
CE	$2N_RN_TS'MKD$
SAD/JAD	$SKN_TNN_R(2KN_T + 7)$

We note that the computational complexity for single or joint antenna detection using the Krylov subspace method is identical for equal Krylov subspace dimensions.

VI. Simulation results

We use the same simulation setup as in [9]. The realizations of the time-variant frequency-selective channel, sampled at the chip rate $1/T_{\mathrm{C}}$, are generated using an exponentially decaying power delay profile with root mean square delay spread $T_{\mathrm{D}} = 4T_{\mathrm{C}} = 1\mu$s for a chip rate of $1/T_{\mathrm{C}} = 3.84 \cdot 10^6\,\mathrm{s}^{-1}$. The autocorrelation for every channel tap is given by the classical Clarke spectrum. The system operates at $f_C = 2\,$GHz and $K = 64$ users move with velocity $v = 70$km/h. For these parameters the Doppler bandwidth is $B = 126$ Hz. The number of subcarriers $N = 64$ and the OFDM symbol with cyclic prefix has length $P = G + N = 79$. The data block consists of $M = 256$ OFDM symbols with $J = 60$ OFDM pilot symbols.

[3]However, in the case where $N \geq KN_T$ or $KN_T \geq NN_R$, the computational complexity of (10) or (15) after matrix inversion lemma would be obtained by permuting the dimensions.

[4]These results are given per iteration of the receiver. However, at the first iteration, no parallel interference cancelation is performed. The multiplicative factor KN_T in the SAD/JAD formula using Krylov disappears.

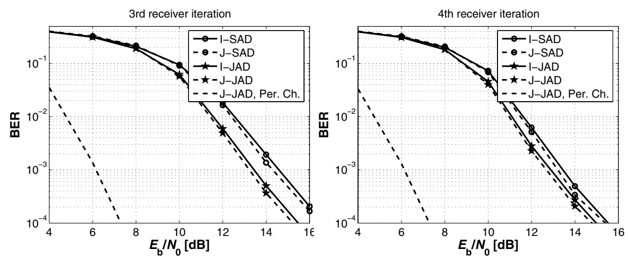

Figure 4: BER using independent(I) or joint (J) encoding at the transmitter with single (SAD) or joint (JAD) antenna detection at the receiver. Both channel estimation and multi-user detection use LMMSE.

The MIMO channel taps are normalized so that

$$\mathbb{E}\left\{\sum_{r=1}^{N_R}\sum_{l=0}^{L-1}|h_{k,t,r}[l]|^2\right\} = 1 \qquad (19)$$

in order to analyze the diversity gain of the receiver only. No antenna gain is present due to this normalization.

A. *Performance Comparison*

In a first step we compare single and joint antenna detection at the receiver combined to independent or joint encoding at the transmitter. The bit error rate (BER) for $N_T = 2$, $N_R = 4$ and $K = N = 64$ is shown in Fig. 4. The channel is LMMSE estimated and multi-user detection is performed using LMMSE filtering. Results are shown after receiver iterations 3 and 4 of the receiver. For comparison we also show the LMMSE performance when the channel is perfectly known. We see that joint antenna detection performs better than single antenna detection. Furthermore, joint antenna detection at the third iteration of the receiver is still better than single antenna detection at the fourth receiver iteration. However, as can be seen in the expression of the filters (10) and (15), the matrix to be inverted for joint antenna detection is N_R times larger than the matrix for single antenna detection. The computational complexity of the exact LMMSE filter grows with N_R^2. A loss of 7dB due to estimation of $KN_T = 128$ channels per receive antenna can be observed.

In a second step, we focus on this optimal solution (joint encoding and joint antenna detection), see Fig. 5. Using the Krylov subspace method, joint antenna detection is implementable with lower computational complexity and storage requirements. Furthermore, less receiver iterations are required. We implement channel estimation (CE) and joint antenna detection (JAD) with LMMSE or by using the Krylov subspace method. We vary the dimensions S and S' of the Krylov subspaces. We also show the LMMSE performance with perfect channel knowledge.

The optimal parameters using a Krylov based receiver are

- for **multi-user detection: time** initialization with a Krylov subspace of dimension $S = 1$,
- for **channel estimation: loop** initialization with a Krylov subspace of dimension $S' = 8$.

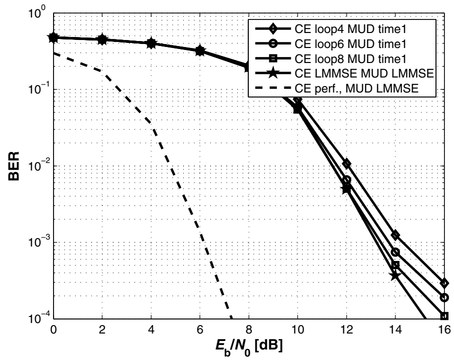

Figure 5: BER using Krylov approximation with **loop** initialization and subspace dimension $S' \in \{4, 6, 8\}$ for CE, and **time** initialization and subspace dimension $S = 1$ for MUD. $N_T = 2$, $N_R = 4$ and $K = N = 64$. We also show the BER with LMMSE detection and perfectly known channel.

We can trade performance against computational complexity by reducing the Krylov subspace dimension.

B. Computational Complexity Comparison

In Fig. 6 we show the computational complexity in number of complex multiplications (CM). We use the Krylov parameters from the optimal results obtained previously: **loop**8 for channel estimation and **time**1 for joint antenna detection.

First we compare the computational complexity for channel estimation using LMMSE or Krylov estimation, per iteration (Fig. 6a). The Krylov subspace method achieves complexity reduction up to more than one magnitude.

Secondly, we compare the computational complexity per receiver iteration for multi-user detection using LMMSE single (SAD) or joint (JAD) antenna detection or Krylov detection in Fig. 6b. Note that both single and joint antenna detection using a Krylov filter have the same complexity per iteration. For the first receiver iteration, complexity reduction of 2 orders of magnitudes is achieved. For the following iterations, the complexity is similar to the LMMSE one.

We have seen in Section A. that the receiver using joint antenna detection requires less receiver iterations than the receiver with single antenna detection for the same performance. The total computational complexity of the receiver (using LMMSE channel estimation and LMMSE multi-user detection) becomes slightly lower with joint antenna detection and 3 receiver iterations than with single antenna detection and 4 receiver iterations, see Fig. 6c. Hence, using the Krylov subspace method for channel estimation and for multi-user joint antenna detection allows consequent computational complexity savings. Fig. 6c shows the complexity for a receiver using either a double LMMSE filter (for channel estimation and multi-user detection) with single or joint antenna detection and for a receiver using a double Krylov approximation. Complexity reduction of up to one order of magnitude is achieved. Furthermore, the computation of the joint antenna detector is parallelized into KN_T branches, thus dividing the computation time by KN_T. In our simulations, $64 \leq KN_T \leq 256$. Finally,

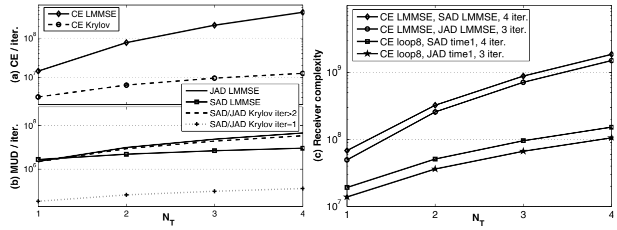

Figure 6: Computational complexity per iteration for CE (a) and MUD (b), and total complexity of the iterative receiver including CE and MUD (c). $N = K = 64$, $M = 256$, $D = 3$, $1 \leq N_T \leq 4$, and $N_R = 4$.

using the Krylov subspace method allows considerable storage requirement reduction [1].

VII. Conclusion

We develop a low-complexity implementation of an LMMSE filter based on the Krylov subspace method. Using this approach for channel estimation and joint antenna detection in a MIMO multi-user time-variant system, we are able to reduce computational complexity by one order of magnitude. Considerable storage requirement reduction is achieved as well as parallelization of the multi-user detection computations into KN_T branches, which is highly beneficial for a low latency hardware implementation.

References

[1] C. Dumard and T. Zemen. Double Krylov subspace approximation for low-complexity iterative multi-user decoding and time-variant channel estimation. In *Proc. IEEE Workshop on Signal Processing Advances in Wireless Com. (SPAWC)*, NYC, USA, June 2005.

[2] C. Dumard and T. Zemen. Integration of the Krylov subspace method in an iterative multi-user detector for time-variant channels. In *Proc. ICASSP*, Toulouse, France, May 2006.

[3] S.V. Hanly and D.N.C. Tse. Resource pooling and effective bandwidths in CDMA networks with multiuser receivers and spatial diversity. *IEEE Trans. Inform. Theory*, 47(4):1328–1351, May 2001.

[4] T. Kailath and A. H. Sayed. *Fast Reliable Algorithms for Matrices with Structure*. SIAM, 1999.

[5] Christoph F. Mecklenbräuker, Joachim Wehinger, Thomas Zemen, Franz Hlawatsch, and Harold Artés. Multiuser MIMO channel equalization. In Thomas Kaiser and André Bourdoux, editors, *Smart Antennas — State-of-the-Art*, EURASIP Book Series, chapter 1.4. Hindawi Publishing Co., 2004.

[6] T. K. Moon and W.C. Stirling. *Mathematical Methods and Algorithms*. Prentice Hall, 2000.

[7] Y. Saad. *Iterative Methods for Sparse Linear Systems*. SIAM, 2nd edition, 2003.

[8] H. van der Vorst. *Iterative Krylov Methods for Large Linear Systems*. Cambridge University Press, 2003.

[9] T. Zemen, C. F. Mecklenbräuker, J. Wehinger, and R. R. Müller. Iterative joint time-variant channel estimation and multi-user detection for MC-CDMA. *IEEE Trans. Wireless Commun.*, 5(6):1469–1478, June 2006.

[10] Thomas Zemen and Christoph F. Mecklenbräuker. Time-variant channel estimation using discrete prolate spheroidal sequences. *IEEE Trans. Signal Processing*, 53(9):3597–3607, September 2005.